Design of Microstrip Dual-Band Filter Using Short-Circuited SIR

M.Shalini, P.Swetha, D,Srilekha, S.Rabia Jebin

***Abstract*— This paper presents the design and implementation of compact dual-band filter with a center frequencies of 2.4 GHz and 5.8 GHz (WLAN) using the short-circuited half-wavelength stepped-impedance resonator (SIR). In the proposed method, the parameters of the SIR are obtained according to the bandwidths and two passband center frequencies of the filter. As a result, the specifications of the dual-band filter can be determined rapidly. The coupling between adjacent SIRs is realized using a short-circuited stub. Compared to the existed dual-band filters, the proposed method is simpler to design. Fourth-order dual-band filter is designed and fabricated to demonstrate the proposed method. Theoretical predictions are verified by the experimental results of the filter.**

***Index Terms*— Bandpass filter (BPF), dual band, microstrip, stepped-impedance resonator (SIR), Short-Circuited Stub, Wireless Local Area Network.**

I. INTRODUCTION

In modern wireless and mobile communication systems, RF/microwave Bandpass filters are essential components. The planar filter has an important role in the RF circuit design, because they can be fabricated using printed circuit technology and are suitable for commercial applications due to their compact size and low cost of integration .Compact, high performance radio frequency (RF) and microwave components capable of operating at more than one frequency band play an important role in a multiband wireless communication system. Recently, due to the increasing demand for dual-band operation in modern RF systems, dual-band filters have become an essential component. Development in wireless communication with dual-band functions has created more potential in global system for mobile communications (GSM), wireless code- division multiple-access (WCDMA), and especially in the newly developed wireless local area networks (WLANs) standards such as IEEE 802.11b/g (2.4/2.45 GHz) and IEEE 802.11a (5.2–5.8 GHz) specifications. The most common method to implement a dual-band filter is to combine two BPFs with individual passbands using additional impedance matching networks [1]. However, this circuit normally has the larger area than twice that of the single-band filter and it may suffer from the extra loss. Therefore, to save the area and cost, it is more appropriate to design an integrated filter capable of operating in two passbands. The cascade connection of a bandpass and a bandstop filter is used to achieve a performance of dual-band filter [2] and the above two passbands could not be far apart from each other, which may be inconvenient in practical applications .The dual-band filter can also be realized using the resonators consisting of the open or short-circuited stubs, which are placed in series or in parallel to create transmission zeros in the middle passband of a wideband BPF [3]–[4]. These circuits have sharp skirt selectivity, but they have a large circuit area due to the many series or shunt stubs and usually require a complex design procedure. In [3]–[4], the stopband rejection is limited since shunt stubs only have narrow bandstop characteristics and there are undesired passbands are present below the first passband and above the second passband. Although the stopband performance can be improved by using series stubs [3], series transmission line components are difficult to realize so that they have to be replaced by coupled- line sections. Another easy method to design dual-band filters is to combine two individual resonators using the common input and output ports [5]. These circuits may have complex structures or occupy a large area. Moreover, the passband frequencies and bandwidths are usually limited since the order of the filter may be difficult to increase. Stub-loaded resonators are also well adopted in the dual-band filter design since they are simple in structure [6]–[7]. However, it is difficult to adjust the coupling coefficient between the resonators to simultaneously meet the dual bandwidth specifications of the filter.

Stepped-impedance resonators (SIRs) have been widely used to realize dual-band filters [8]–[9]. The SIR is very attractive and suitable to design filters due to its controllable resonant frequencies, simple structure, and well-established design. However, the first step of the conventional method to design a SIR dual-band filter is to draw the design graphs of coupling coefficients for each pair of SIRs. To find each point on the design graph, full-wave electromagnetic (EM) simulation software should be used to calculate the coupling coefficient. Since the coupling between adjacent SIRs is via coupled-line sections. As a result, it is very time consuming to construct design graphs. Furthermore, as the order of the filter is larger than three, more than one design graph is required. This method might be inefficient to design a dual-band filter more than fourth order. Although there are many studies and experiments related to SIR dual-band filters, there still lacks an efficient and time-saving design method.

In this paper, we present an easy, simple and time-saving procedure to design a SIR dual-band filter. Here, a short-circuit terminated half-wavelength SIR is used. First,

Manuscript received April 24, 2015.

M.Shalini, ECE , Velammal Engineering College , Chennai, India, 9677280805.

P.Swetha, ECE, Velammal Engineering College, Chennai, India, 7418200764.

D.Srilekha, ECE , Velammal Engineering College , Chennai, India, 9952068596.

S.Rabia Jebin, ECE , Velammal Engineering College , Chennai, India, 7667809031.

the structural parameters of the SIR can be determined according to the two center frequencies and bandwidths of the dual-band filter. The coupling between adjacent SIRs is then realized by a short-circuited stub, which acts as a K-inverter. The method shown here is very different from those in [8]–[9], where the coupling coefficient and the available bandwidth are limited by the preselected SIR structure. In addition, by using the short-circuited stub, the coupling strength between SIRs is much less constrained compared to coupled-line sections, since the gap between coupled lines is limited. The proposed method follows the common design procedure[10], namely, determining the filter specifications first and then choosing appropriate resonator structures. On the basis of this method, a dual-band filter can be quickly realized and simulated using the circuit simulator, especially for a high-order dual-band filter.

II. SHORT-CIRCUITED HALF-WAVEMENGTH SIR CHARACTERISTICS

The SIR has an ability to control the first and second resonant frequencies of the filter [11]. The short-circuit terminated half wavelength SIR, where Z_1 and Z_2 are the characteristic impedances of the microstrip sections θ_1 and θ_2 are the respective electrical lengths shown in Fig 1.

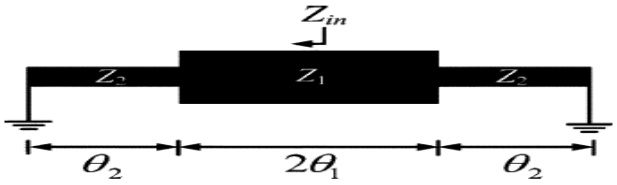

Fig. 1. Structure of the short-circuit terminated half-wavelength SIR

The input impedance (1) seen from the middle of the SIR is

$$Z_{in} = jZ_1 \frac{Z_2 \tan\theta_2 - Z_1 \tan\theta_1}{Z_1 - Z_2 \tan\theta_1 \tan\theta_2} \qquad (1)$$

Therefore, the fundamental frequency (f_1) and the first spurious frequency (f_2) of the SIR are determined by the following equations:

$$R\tan\theta_1 \ \tan\theta_2 - 1 = 0, \text{ for } f_1 \qquad (2)$$

$$R\tan\theta_2 + \tan\theta_1 = 0, \quad \text{for } f_2 \qquad (3)$$

Where $R=Z_1/Z_2$ is the impedance ratio of the SIR. If $f_2 \geq 2f_1$ is required, $R\geq 1$ should be chosen and vice versa. Thus, the passband center frequencies of the dual-band filter (i.e., f_1 and f_2) can be controlled by the impedance ratio R and the electrical length ratio of θ_1 and θ_2 .

III. DESIGN PROCESS OF THE DUAL-BAND FILTER

In this method, there are N resonators in the N^{th}-order filter. Fig. 2(a) shows a generalized BPF circuit using impedance inverters [12]. The series resonant circuit can be replaced by a short-circuit terminated half-wavelength SIR.
Submit your manuscript electronically for review.
Final Stage The configuration of the n^{th} resonator in the proposed filter is shown in Fig. 2(b) and (c).

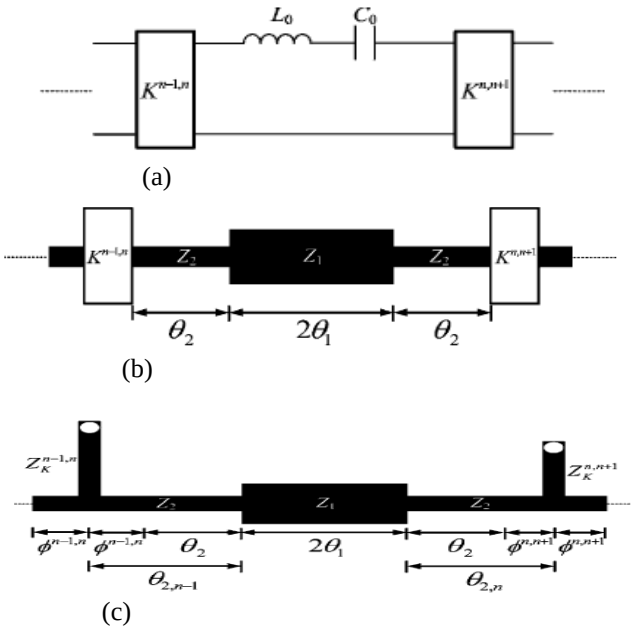

Fig. 2. Configuration of the nth resonator in the proposed filter. (a) BPF circuit with series resonators and impedance inverters. (b) Dual-band filter using short-circuit terminated half-wavelength SIRs and K-inverters (c) Microstrip implementation of the dual-band filter.

The coupling between the n^{th} and $(n+1)^{th}$ resonators is represented by the K-inverter (i.e., $K^{n,n+1}$). Since all resonators in the filter have the same structure, their reactance slope parameters x [12] are equal at the specific frequency. In the process, first, the filter specifications center frequencies and bandwidths are given. Choose a proper set of SIR structural parameters that respect to two passband center frequencies and reactance slope parameters. The value of the K-inverter between SIRs is then calculated according to each passband bandwidth. The K-inverter is implemented by a short-circuited stub and its parameters can be obtained by the given design equations. Finally, by combining the SIRs and K-inverters along with the proper input and output ports, the dual-band filter is completed. Here g_0, g_n and g_{n+1} are the element values of the low-pass filter prototype.

A. K-Inverter

The short-circuit terminated half-wavelength SIR is adopted in the filter, the short-circuited stub can be straight forwardly used as the K-inverter between resonators. Each K-inverter value corresponding to the filter specifications is obtained as [12]

$$K^{n,n+1} = \Delta\sqrt{\frac{x^2}{g_n g_{n+1}}} \qquad (4)$$

Fig. 3(a) shows an equivalent K-inverter circuit where a shunt Susceptance $b^{n,n+1}$ is included. The shunt susceptance can be implemented by a microstrip short-circuited stub, as shown in Fig. 3(b). In Fig. 3(b), Z_d and $Z_K^{n,n+1}$ are the characteristic impedances of the input/output transmission line and the short-circuited stub, respectively, while $\phi^{n,n+1}$ and $\psi^{n,n+1}$ are the respective electrical lengths.

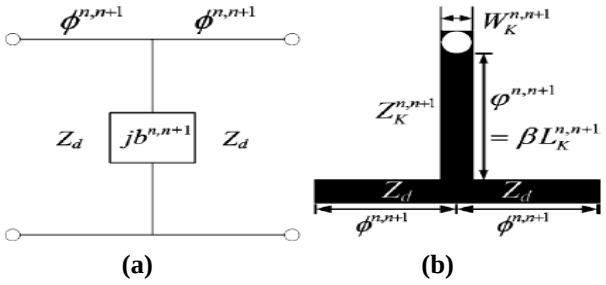

Fig.3. (a) Equivalent circuit model of the K-inverter. (b) Microstrip realization of the K-inverter.

By comparing the ABCD matrix, the relations between the K-inverter and its equivalent circuit are obtained as [12]

$$K^{n,n+1} = Z_d \tan|\Phi^{n,n+1}| \quad (5)$$

$$b^{n,n+1} = \frac{(K^{n,n+1}/z_d)^2 - 1}{K^{n,n+1}} \quad (6)$$

$$\Phi^{n,n+1} = -\frac{1}{2}\tan^{-1}\left|\frac{2}{b^{n,n+1} z_d}\right| \quad (7)$$

Neglecting the T-junction effect in Fig. 3(b), the shunt susceptance can be derived as

$$jb^{n,n+1} = -j\frac{1}{Z_K^{n,n+1}}\cot(\varphi^{n,n+1}) \quad (8)$$

$$jb^{n,n+1} = -j\frac{1}{Z_K^{n,n+1}}\cot\left(\beta L_K^{n,n+1}\right) \quad (9)$$

Where $\beta = \omega\sqrt{\mu\epsilon}$ is the propagation constant. In Fig. 3(b), the higher the impedance Z_d is (i.e., narrower linewidth), the smaller the T -junction effect is. For simplicity, we ignore the influence of the T-junction effect on the K-inverter in the following discussion.

In this paper, we choose $Z_d = Z_2$ since the K-inverter is connected to the end of the SIR. For the dual-band filter, since β is dependent on the operating frequency, from (6) and (8), the K-inverter in Fig. 3 leads to different K values in two passbands (i.e.,$K_1^{n,n+1}$ for the first passband and $K_2^{n,n+1}$ for the second passband). Moreover, the longer the length $L_K^{n,n+1}$is, the larger the values $K_1^{n,n+1}$ and $K_2^{n,n+1}$ are. It should be noted that in the practical application, the ratio K of values is approximately equal to the ratio of center frequencies.

$$\frac{f_1}{f_2} = \frac{\beta_1}{\beta_2} \approx \frac{K_2^{n,n+1}}{K_1^{n,n+1}} \quad (10)$$

$$\Phi^{n,n+1} \approx -\frac{Z_K^{n,n+1}\ \beta L_K^{n,n+1}}{z_d} \quad (11)$$

B. SIR Structural Parameters Determination

In this paper, to simplify the design process [12], the element values of the low-pass filter prototype for two passbands are chosen to be identical (i.e., the same ripple level for two passbands). Thereby, from (4), the ratio of the fractional bandwidths is calculated as

$$\frac{\Delta_2}{\Delta_1} = \frac{K_2^{n,n+1}}{K_1^{n,n+1}}\ \frac{x_1}{x_2} \quad (12)$$

where Δ_1 and Δ_2 is the fractional bandwidth for the first passband and the second passband respectively. x_1 and x_2 are the reactance slope parameters seen from one end of the SIR at $f_1$and f_2 , respectively.

IV. Design Procedure

In this method, one fourth-order dual-band filter with f_2/f_1 smaller than 2 was designed and implemented. This filter has a Chebyshev frequency response with a 0.1dB ripple level. The circuit was fabricated on the Rogers RO4003 substrate with a dielectric constant of 3.6, a loss tangent of 0.0021, and a thickness of 0.508 mm. Each via-hole has a diameter of 0.2 mm.

The simulation was carried out using a commercially available full-wave EM simulation tool (Advanced Design System). The final layout of the completed filter, including the physical dimensions, is shown in Fig. 4.The measurements were carried out using an Agilent network analyzer.

A. Steps Involved In Designing Dual Band Filter

The steps involved in designing the dual band filter flow graph as shown in Fig. 4 and are explained below:

Step 1: Identify the dual-band filter specifications, including the center frequencies (f_1, f_2), the fractional bandwidths (Δ_1, Δ_2), and the filter order (N).
Step 2: x_1/x_2 is calculated using the equation 12. θ_1 and θ_2 are obtained for $f=f_1$.We choose Z_2 first and then Z_1 is determined by R.

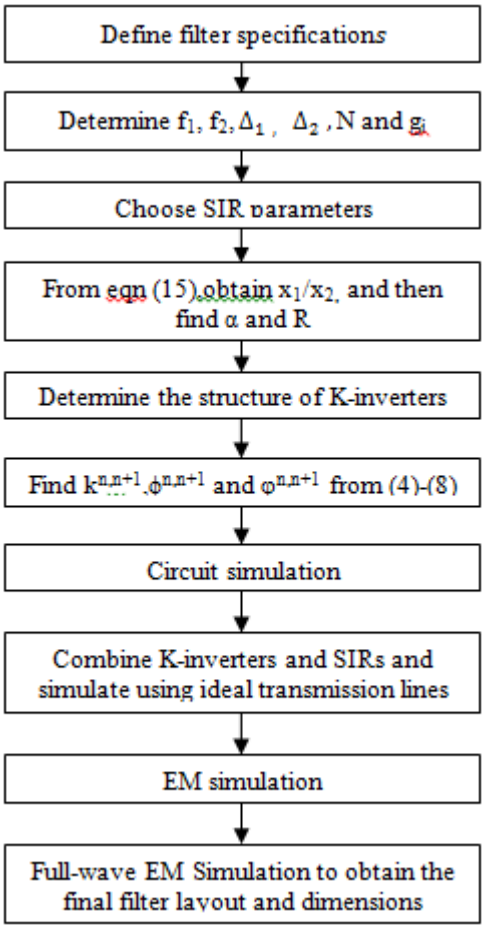

Fig. 4. Design flowchart of the proposed method

Step 3: By using the impedance and electrical length value the structural parameter of the SIR and the *K*-inverter is obtained by using the line calculator in the ADS.

Step 4: Combine the *K*-inverters and SIRs.θ_2, $n=\theta_2+\phi^{n,\ n+1}$. The input and output ports are designed using the method in [12]. As a result, the response of the filter with ideal transmission lines (i.e., the inverters are also made of ideal transmission lines) can be simulated in the circuit simulator.

Step 5: Replace the ideal transmission line with the microstrip line and slightly fine tune the filter dimensions for optimal performance in the circuit simulator. Finally, the filter with the fine-tuned dimensions in the circuit simulator is simulated with a full-wave EM simulator to take the effects of via-holes, discontinuities, and junctions into account. Then the dual band filter is designed using ADS tool.

B. Fourth- Order Dual Band Filter

A fourth-order dual-band filter with the center frequencies f_1=2.4 GHz and f2= 5.8 GHz (i.e., $f_2/ f_1 > 2$). The fractional bandwidths of the two passbands are Δ_{21} = 0.14 and Δ_2 =0.08. For the fourth-order filter, the element values of the low-pass filter prototype are g_0=1, g_1 =1.1088, g_2 =1.306, g_3 =1.770, g_4 =0.817 and g5 =1.345. Applying (15), we have f_2/f_1 = 2.41 and x_1/x_2 = 0.236 are obtained .From Fig. 6, the structural parameters of the SIR are found to be R=2.43 and α = 0.55. In this example, Z_2 =Z_d =84Ω are chosen so that Z_1 =34.567 for R= 2.43.

The K-inverters between resonators for the first and second passbands are calculated based on the design procedure. Fig. 5 shows the final physical layout and dimensions of the proposed dual-band filter.

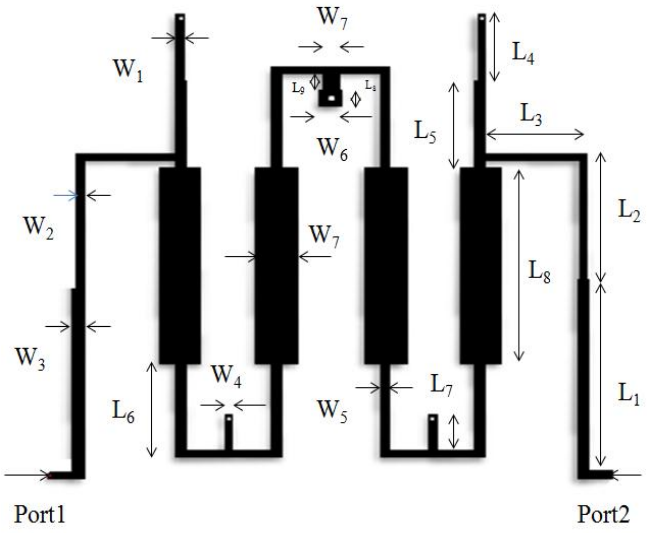

Fig. 5. Layout of the proposed fourth-order dual-band filter.

Filter dimensions in mm: W_1=0.3105, W_2=0.3302, W_3=0.4572, W_4=0.261, W_5=0.381, W_6=1.0279 and W_7=0.6096. L_1=12.448, L_2=7.32094, L_3=4.0894, L_4=4.30272, L_5=4.80272, L_6=5.715, L_7=2.1294, L_8= 12.67968and L_9=1.1279.

Figure 6 shows a photograph of the fabricated dual-band filter. The size of the filter is 30.2626 mm X 24.5482 mm. Figure 8 shows the simulated and measured responses. Futhermore, the losses are improved by tuning the SIR parameters. Figure 8 shows the measured results for the first passband, the center frequency is 2.1942 GHz. The minimum insertion loss is 0.3 dB and the return loss is better than 20 dB. The measured 3dB fractional bandwidth is 16.57% from 1.899 to 2.242 GHz. The passband group-delay variation is 0.8 ns. The 3D view of the proposed UWB filter structure is shown in the fig 7.

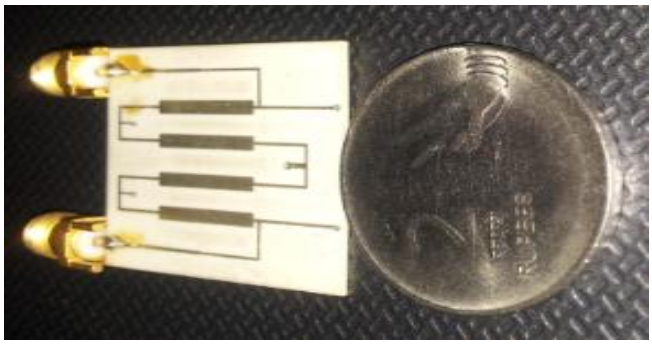

Fig. 6. Photograph of the fabricated fourth-order dual-band filter

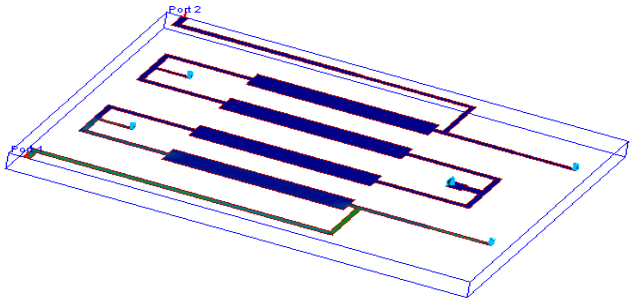

Fig. 7. Isometric view – 3D view

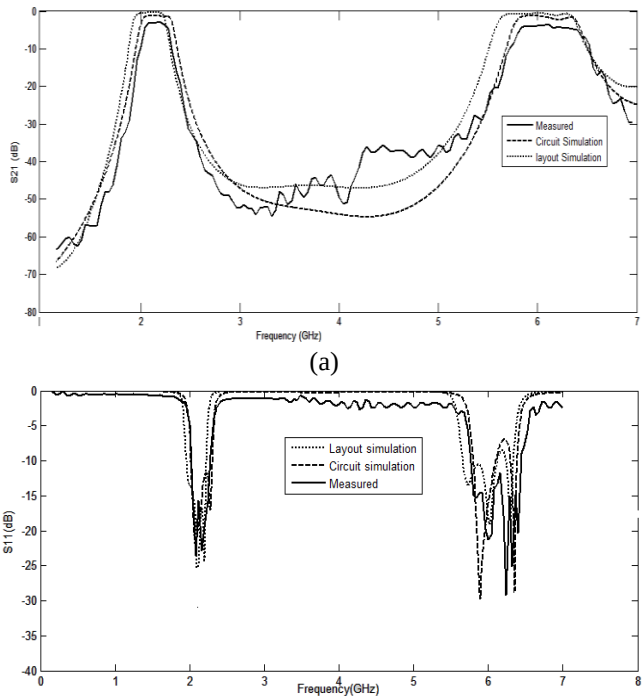

Fig. 8. Simulated and measured results of the fourth order dual-band filter (a) S_{21} Response (b) S_{11} Response

For the second passband, the center frequency is 5.9875 GHz. The minimum insertion loss is 0.8 dB and the return loss is better than 15 dB. The measured 3-dB fractional bandwidth is 13.97% from 5.569 to 6.406 GHz. The passband group-delay variation is 0.6 ns shown in Fig 8.

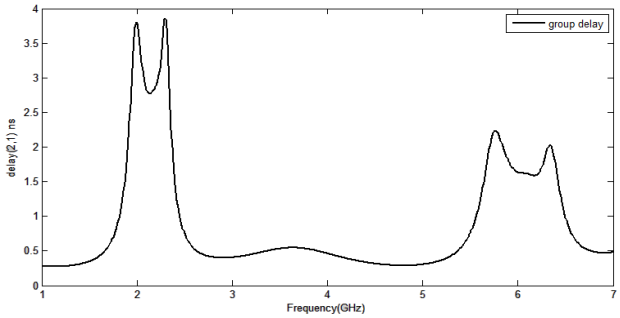

Fig. 9. Group delay for the first passband and the second passband.

However, if the transmission lines can be placed close to each other, the area occupied could be reduced which makes the filter compact. In order to make the filter compact, meandering of the resonator is carried out. This structure is illustrated in Fig.9.

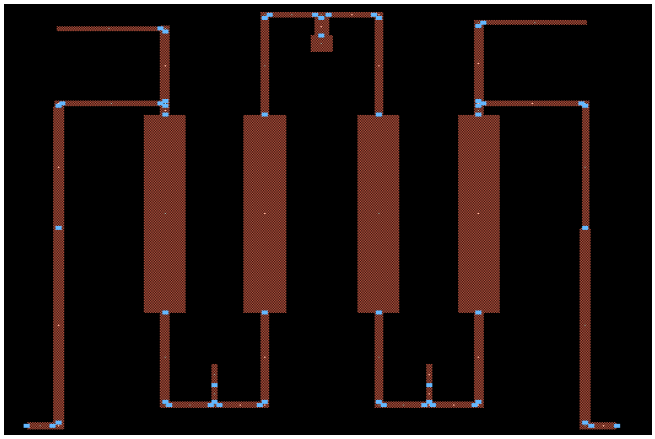

Fig. 9. Layout of the meandered fourth-order dual-band filter

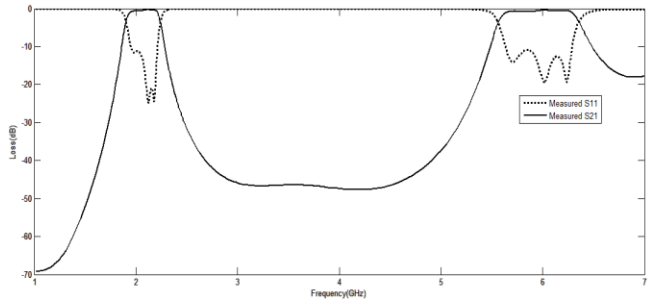

Fig. 10. Simulated results of the meandered fourth order dual-band filter

This approach leads to a filter size of (26 x 24) mm is shown in fig 9. The rejection between the two passbands is better than 40 dB from 2.4 to 5.4 GHz. The minimum insertion loss is (0.2 -0.3) dB and the return loss is better than 20 dB is shown in figure.10 for the center frequencies 2.2GHz and 5.8GHz respectively.

V. CONCLUSION

In this work, a simple method to design dual-band filters has been presented. The short-circuited half-wavelength SIR is used to realize a filter with dual passbands. The coupling between adjacent SIRs is easily realized by a short-circuited stub. In this design, the narrow gap between resonators is avoided so that the filter specifications are less constrained. Due to the design equations in the proposed method, the filter can be first simulated using the EM simulator. The proposed method follows the regular design process and is very appropriate to apply to the relatively high-order dual-band filters. A fourth-order dual-band filter was constructed to demonstrate the proposed method. Good agreement between measured and simulated results is observed.

ACKNOWLEDGMENT

The preferred spelling of the word “acknowledgment” in American English is without an “e” after the “g.” Use the singular heading even if you have many acknowledgments. Avoid expressions such as “One of us (S.B.A.) would like to thank ... .” Instead, write “F. A. Author thanks ... .” **Sponsor and financial support acknowledgments are placed in the unnumbered footnote on the first page**.

REFERENCES

[1] H. Miyake, S. Kitazawa, T. Ishizaki, T. Yamada, and Y. Nagatomi, “A miniaturized monolithic dual band filter using ceramic lamination technique for dual mode portable telephones,” in IEEE MTT-S Int. Microw. Symp. Dig., vol. 2, pp. 789–792, Jun. 1997.

[2] L. C. Tsai and C. W. Hsue, “Dual-band bandpass filters using equallength coupled-serial-shunted lines and □-transform technique,” IEEE Trans. Microw. Theory Tech., vol. 52, no. 4, pp. 1111–1117, Apr. 2004.

[3] C. M. Tsai, H. M. Lee, and C. C. Tsai, “Planar filter design with fully controllable second passband,” in IEEE Trans. Microw. Theory Tech., vol. 53, no. 11, pp. 3429–3439, Nov. 2005.

[4] H. M. Lee and C. M. Tsai, “Dual-band filter design with flexible passband frequency and bandwidth selections,” IEEE Trans. Microw. Theory Tech., vol. 55, no. 5, pp. 1002–1009, May 2007..

[5] X. Y. Zhang, J. Shi, J. X. Chen, and Q. Xue, “Dual-band bandpass filter design using a novel feed scheme,” in IEEE Microw. Wireless Compon. Lett., vol. 19, no. 6, pp. 350–352, Jun. 2009.

[6] P. Mondal and M. K. Mandal, “Design of dual-band bandpass filters using stub-loaded open-loop resonators,” in IEEE Trans. Microw. Theory Tech., vol. 56, no. 1, pp. 150–155, Jan. 2008.

[7] M. Zhou, X. Tang, and F. Xiao, “Compact dual band bandpass filter using novel E-type resonators with controllable bandwidths,” in IEEE Microw. Wireless Compon. Lett., vol. 18, no. 12, pp. 779–781, Dec. 2008.

[8] C. H. Tseng and H. Y. Shao, “A new dual-band microstrip bandpass filter using net-type resonators,” IEEE Microw.Wireless Compon. Lett., vol. 20, no. 4, pp. 196–198, Apr. 2010.

[9] F. C. Chen and Q. X. Chu, “Novel multistub loaded resonator and its application to high-order dual-band filters,” IEEE Trans. Microw. Theory Tech., vol. 58, no. 6, pp. 1551–1556, Jun. 2010.

[10] Wei-Shin and Chi-Yang, “Analytical design of microstrip short-circuit terminated stepped impedance resonators dual band filters,” IEEE Trans. Microw. Theory Tech., vol. 59, no. 7, pp. 1730–1739, July.2011.

[11] M. Makimoto and S. Yamashita, Microwave Resonators and Filters for Wireless Communication: Theory, Design and Application. Berlin, Germany: Springer-Verlag, 2001.

[12] G. L. Matthaei, L. Young, and E. M. T. Jones, Microwave Filters, Impedance-Matching Networks and Coupling Structures. Norwood, MA: Artech House, 1980.